On the Contraction of Excitable Systems

Alessandro Cecconi^{1,2}, Michelangelo Bin¹, Lorenzo Marconi¹, Rodolphe Sepulchre^{2,3}

Abstract—We analyze contraction in conductance-based excitable systems and link it to reliable spike timing. For a Hodgkin-Huxley neuron with synaptic input, we prove the unforced dynamics is incrementally exponentially stable on a compact physiological set. With impulsive inputs, contraction persists under an average dwell-time condition, and for periodic spike trains we derive an explicit lower bound on the interimpulse period. In the high-rate limit the synapse is effectively held open, the conductance is nearly constant, and self-sustained limit-cycle oscillations can arise, so contraction no longer holds. This continuous-time view explains when spike times extracted by an event detector remain robust across trials, and simulations confirm both regimes.

I. INTRODUCTION

Excitable systems, exemplified by conductance-based models, mix the continuous and the discrete. Their trajectories follow differential equations but consist of sequences of discrete events [1]. Building on this mixed description, neuromorphic control exploits excitable internal models to achieve event regulation, rather than trajectory regulation. Internal event generators can synchronize with external events despite a persistent mismatch between the corresponding continuous-time trajectories [2], [3]. In neuroscience, reliability refers to the trial-to-trial reproducibility of spike times under the same input stimulation, with output spike voltages that lock to input synaptic currents despite variability in initial conditions and other perturbations [4]-[6]. The objective of this work is to show that an excitable behavior becomes contractive when regarded as an event generator, meaning that the input current keeps the state variables near an exponentially stable equilibrium except for brief spikes, that is, short and sharp excursions separated by refractory periods. In this setting, the continuous contraction property of the flow explains the discrete reliability of the observed

Contraction theory formalizes robustness as incremental exponential convergence of trajectories driven by the same input [7]–[9]. In excitable dynamics contraction is input dependent [10], [11]. Constant or effectively constant inputs can generate limit-cycle oscillations that are not contractive and that remain sensitive to phase perturbations [12]–[14]. In contrast, subthreshold inputs, or event inputs that trigger spikes without holding the system away from its stable rest, result in contracting behavior with trajectories that draw

together and with spike times that align up to bounded timing variability. This input-selective viewpoint clarifies how the very same neuron can appear phase-sensitive in a tonic regime yet display highly reproducible timing when driven by sparse triggering signals.

We formalize this viewpoint on a standard conductance-based formulation with gating dynamics and a first-order synaptic state. Physiological bounds on voltage and gates define a compact forward-invariant set on which the unforced Hodgkin–Huxley flow is incrementally exponentially stable. To connect the continuous flow with discrete observations we pair the model with an event detector that maps presynaptic spike trains to post-synaptic spike times. When the flow is contractive, different initial conditions under the same admissible input lead to trajectories that converge and to event sequences that coincide after a short transient.

We then study impulsive synaptic drives and identify conditions under which contraction, and therefore event-level reliability, persists. For general spike trains, an average dwell-time requirement ensures impulses are sufficiently spaced so that the state returns near equilibrium between events. For periodic spike trains, this requirement becomes a lower bound on the inter-impulse period that depends on the contraction margin of the unforced flow. The opposite regime reveals the limits of reliability. At high input rates the synaptic state saturates, the effective conductance becomes nearly constant, and the neuron may enter self-sustained periodic firing on a limit cycle, which destroys global contractivity and makes timing sensitive to phase.

Numerical experiments on a Hodgkin–Huxley neuron illustrate both behaviors predicted by the analysis. With adequately spaced inputs, trajectories contract and spike times lock tightly after a brief transient. With high-rate drives, tonic oscillations exhibit persistent phase offsets across trials and timing variability does not shrink. Together these findings provide a simple and testable account of when excitable systems are contractive at the level of events and why their spike timings can be robust in practice.

II. MODELING EXCITABLE SYSTEMS

We consider excitable systems modeled by the following conductance-based model

$$\tau_{j}(v)\dot{x}_{j} = -x_{j} + \mu_{j}(v), \qquad j = 1, \dots, m,$$

$$C\dot{v} = -\bar{g}_{\text{leak}}(v - E_{\text{leak}}) - \sum_{k=1}^{n} i_{k}(x, v) + i_{s},$$
(1)

where $v \in \mathbb{R}$ is the membrane voltage, and $x_j \in \mathbb{R}$ are gating variables. The functions $\mu_j : \mathbb{R} \to (0,1)$ and $\tau_j : \mathbb{R} \to \mathbb{R}_+$ are the steady-state activation and the voltage-dependent

Alessandro Cecconi, Michelangelo Bin, and Lorenzo Marconi are with the Department of Electrical, Electronic and Information Engineering (DEI), University of Bologna, Bologna, Italy.

² Alessandro Cecconi and Rodolphe Sepulchre are with STADIUS, Department of Electrical Engineering (ESAT), KU Leuven, Leuven, Belgium.

³ Rodolphe Sepulchre is with the Department of Engineering, University of Cambridge, Cambridge, United Kingdom.

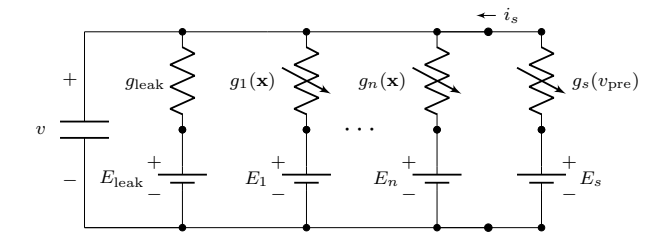


Fig. 1: Circuit schematic of the conductance-based model (1) with the external synapse (2).

time constant, respectively. These functions typically have a sigmoidal shape [13, Sec. 1.8].

The quantities $i_k(x,v)$ represent internal ionic currents. They have an Ohmic form

$$i_k(x,v) = \bar{g}_k \varphi_k(x) (v - E_k), \qquad k = 1,\ldots,n,$$

where $\bar{g}_k > 0$ is the maximal conductance, $E_k \in \mathbb{R}$ the corresponding reversal potential, and $\varphi_k : \mathbb{R}^m \to (0,1)$ is an activation function determining the fraction of open channels.

The variable i_s denotes an external synaptic current, which is modeled by

$$\dot{s} = -\frac{1}{\tau_s}s + \alpha(1-s)v_{\text{pre}}(t), \quad i_s(t) = -\bar{g}_s s(v - E_s),$$
 (2)

where $\alpha \in (0,1]$, $\tau_s > 0$ is the synaptic time constant, $\bar{g}_s > 0$ is the maximal synaptic conductance, $E_s \in \mathbb{R}$ is the synaptic reversal potential, and $v_{\text{pre}}(t)$ is the pre-synaptic voltage, the model input. The synapse is a one-port element of the same type as the internal currents.

We model pre-synaptic spikes by a locally finite set of times. Let

$$\mathbb{U} := \{ I \subseteq [0, \infty) : \forall T > 0, \operatorname{card}(I \cap [0, T]) < \infty \}.$$

Each $\mathcal{I} \in \mathbb{U}$ admits a unique strictly increasing sequence $\mathcal{I} = \{t_\ell\}_{\ell=1}^N$ with $N \in \mathbb{N}$. With each \mathcal{I} we associate the spike-train signal

$$v_{\text{pre}}(t) \coloneqq \sum_{t_{\ell} \in \mathcal{T}} \delta(t - t_{\ell}),$$
 (3)

where δ is the Dirac distribution. If $t_{\ell} = \ell T$, then the spike train is periodic. This representation is standard in neuroscience and neuromorphic engineering [14], [15].

The Hodgkin–Huxley model [16] is obtained as a particular case for m=3 gates modulating n=2 currents

$$i_{\text{Na}} = \bar{g}_{\text{Na}} x_1^3 x_2 (v - E_{\text{Na}}), \qquad i_{\text{K}} = \bar{g}_{\text{K}} x_3^4 (v - E_{\text{K}}),$$

with $i_{\rm Na}$, and $i_{\rm K}$ representing the sodium and potassium current, respectively. The equivalent circuit is shown in Figure 1.

In physiological conditions, neurons have a well-defined resting state, which corresponds to a unique stable equilibrium. Furthermore, the membrane voltage remains confined in an interval determined by the minimum and maximum of the reverse potentials, that is, in the case of the Hodgkin-Huxley, the Nernst potential of potassium and the Nernst potential of sodium, respectively [12]. We link such conditions to our model (1)-(2). With $v_{\rm pre}\equiv 0$, the unforced voltage dynamics in (1) can be rewritten as

$$C\dot{v} = -G(x,s)(v - E(x,s)),\tag{4}$$

where

$$G(x,s) := \bar{g}_{\text{leak}} + \sum_{k=1}^{n} \bar{g}_{k} \varphi_{k}(x) + \bar{g}_{s} s \ge \bar{g}_{\text{leak}} > 0, \quad (5)$$

and

$$E(x,s) := \frac{\bar{g}_{\text{leak}} E_{\text{leak}} + \sum_{k} \bar{g}_{k} \varphi_{k}(x) E_{k} + \bar{g}_{s} s E_{s}}{\bar{g}_{\text{leak}} + \sum_{k} \bar{g}_{k} \varphi_{k}(x) + \bar{g}_{s} s}.$$
 (6)

Hence, E(x,s) is a convex combination of reversal potentials. In particular, let $E_{\min} := \min\{E_{\text{leak}}, E_k, E_s\}$, and $E_{\max} := \max\{E_{\text{leak}}, E_k, E_s\}$. Then, for every (x, v), it holds

$$E(x,s) \in [E_{\min}, E_{\max}].$$

For instance, for the Hodgkin–Huxley model one has $E(x,s) \in [E_{\rm K},E_{\rm Na}]$, provided that $E_{\rm s} \in (E_{\rm K},E_{\rm Na})$. More in general, one can show the following.

Lemma 1. With S = [0, 1], $\mathcal{X} = [0, 1]^m$, $\mathcal{V} = [E_{\min}, E_{\max}]$, define $\mathcal{Z} := S \times \mathcal{X} \times \mathcal{V}$. Then, \mathcal{Z} is compact and forward invariant for (1)–(2) under (3).

Proof. See Appendix.

As for the rest state, we notice that an equilibrium (s^*, x^*, v^*) of (1)–(2) with $v_{\rm pre} \equiv 0$, necessarily satisfies $s^*=0$, and the current balance

$$\bar{g}_{\text{leak}}(v^* - E_{\text{leak}}) + \sum_{k=1}^n \bar{g}_k \varphi_k(x^*)(v^* - E_k) = 0.$$
 (7)

Assuming, as customary, $v^* = 0$ (which can be done without loss of generality by appropriately re-defining the reverse potentials), we obtain $x_j^* = \mu_j(0)$, and (7) reduces to

$$\bar{g}_{\text{leak}} E_{\text{leak}} + \sum_{k=1}^{n} \bar{g}_k \varphi_k(x^*) E_k = 0, \tag{8}$$

Namely, $\bar{g}_{\text{leak}}E_{\text{leak}}$ compensates for the residual reversal potentials at x^* , ensuring that $(s^*, x^*, v^*) = (0, x^*, 0)$ is an equilibrium for (1)-(2).

For the sake of compactness, we rewrite (1)–(2) as

$$\dot{z} = F(z) + G(z) u, \quad z(0) = z_0,$$
 (9)

where $z := \operatorname{col}(s, x, v) \in \mathcal{Z}, u := v_{\operatorname{pre}}$, and

$$F(z) := \operatorname{col} \left(-\tau_s^{-1} s, \ f(z) + g(z) s \right),$$

$$G(z) := \operatorname{col} \left(\alpha (1 - s), \ \mathbf{0}_{m+1} \right),$$

$$g(z) := \operatorname{col} \left(\mathbf{0}_m, -(\bar{q}_s/C)(v - E_s) \right),$$

and where f(z) collects the intrinsic unforced conductance—based dynamics of x and v in (1).

While the previous conditions do not by themselves imply uniqueness of the rest state, assuming a unique attractive and locally exponentially stable equilibrium is both standard in the literature and well supported empirically for conductance-based neuron models [12]. We therefore adopt the following.

Assumption 1. $z^* := (0, x^*, 0)$ is the unique equilibrium of (9) with $u \equiv 0$, and it is locally exponentially stable (LES) with a domain of attraction including \mathcal{Z} .

Indeed, for (9) without a constant bias $(u(t) \not\equiv \bar{u})$, the resting equilibrium is typically unique. When a constant current is introduced and tuned past a critical value, the rest state either loses stability or disappears via a bifurcation, and a stable periodic orbit becomes the attracting behavior [17]. Under Assumption 1, z^* is also exponentially stable on \mathcal{Z} , as established by the following lemma.

Lemma 2. If an equilibrium $z^* \in \mathcal{Z}$ for (9) with $u \equiv 0$ is locally exponentially stable and attractive on a compact forward-invariant set \mathcal{Z} , then z^* is exponentially stable on \mathcal{Z} .

Proof. See Appendix.

We now want to characterize the discrete-event model associated with the dynamical system (9), by extracting events from the continuous-time trajectory. Given $z_0 \in \mathcal{Z}$ and $\mathcal{I} \in \mathbb{U}$, let $\varphi(t,z_0,\mathcal{I})$ denote the solution of (9) driven by (3), and let $v(t,z_0,\mathcal{I})$ be its voltage component.

We define a hysteretic *event detector* by fixing thresholds $0 < v_{\rm low} < v_{\rm high}$, and a dwell time $\tau_{\rm e} > 0$, chosen on the order of the time constant of the positive feedback current (in Hodgkin–Huxley, the sodium activation timescale). For a C^1 signal v, a closed interval [a,b] with a < b is *admissible* if

- (i) $v(s) > v_{\text{high}}$ for all $s \in (a, b)$,
- (ii) $b-a \geq \tau_e$,
- (iii) $\exists \epsilon_{\pm} > 0$ such that $v(t) \leq v_{\text{low}}$ on $(a \epsilon_{-}, a) \cup (b, b + \epsilon_{+})$. Define the temporal set of admissible intervals

$$\mathcal{T}[v] := \{[a, b] : a < b \text{ and (i)-(iii)}\},$$

and the set of (apex) event times

$$\mathcal{D}[v] := \left\{ \min \arg \max_{s \in I} v(s) : I \in \mathcal{T}[v] \right\} \subset \mathbb{R}.$$
 (10)

On any bounded interval with finitely many impulses, $\mathcal{D}[v]$ is finite. Only $v > v_{\text{high}}$ defines an admissible window, and the band $[v_{\text{low}}, v_{\text{high}})$ is used solely to reset. This detector can be considered a Schmitt-trigger (hysteresis via $v_{\text{low}} < v_{\text{high}})$ with an added dwell-time τ_{e} . Then, the input-output event model is defined as

$$\mathcal{F}: \mathcal{Z} \times \mathbb{U} \to \mathbb{U}, \quad \mathcal{F}(z_0, \mathcal{I}) := \mathcal{D}[v(\cdot, z_0, \mathcal{I})], \quad (11)$$

for fixed detector parameters $(v_{\text{low}}, v_{\text{high}}, \tau_{\text{e}})$.

A block diagram of the overall architecture is shown in Figure 2. In the following, we will say that the discrete-event system is *reliable* if the underlying forced continuous dynamics is contractive. This inherits the robustness properties implied by contraction, such as robustness to disturbances and parameter uncertainties.

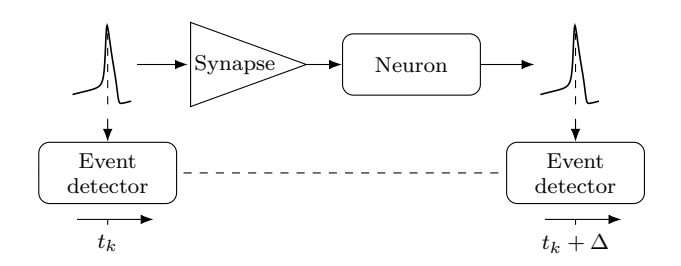


Fig. 2: Block diagram of the overall architecture. A spike is converted into a timing through an event detector.

III. CONTRACTION PROPERTIES OF EXCITABLE SYSTEMS

In this section we show the main results of the paper, proving contraction of the unforced system (9), and showing how the property is maintained by certain inputs of interest.

Definition 1 (Incremental Exponential Stability). Let \mathcal{Z} be a compact forward invariant set for (9). The system (9) with $u \equiv 0$ is said to be incrementally exponentially stable (IES) on \mathcal{Z} if there exist $k \geq 1$, and $\lambda > 0$ such that, for all $z_1, z_2 \in \mathcal{Z}$,

$$\|\varphi(t, z_1) - \varphi(t, z_2)\| \le ke^{-\lambda t} \|z_1 - z_2\| \quad \forall t \ge 0.$$

It is known that incremental stability and uniform convergence coincide on compact sets [18]. Therefore, if system (9) is IES on \mathcal{Z} with $u \equiv 0$, it posses a unique exponentially stable steady-state solution in \mathcal{Z} . In our case, it coincides with the unique exponentially stable equilibrium. The next statement upgrades the pointwise stability to an incremental estimate on the whole set, hence to contraction of the unforced flow.

Theorem 1. Under Assumption 1, consider (9) with $u \equiv 0$ on the forward-invariant set \mathcal{Z} . Let $z^* \in \mathcal{Z}$ be the unique equilibrium of (9), exponentially stable on \mathcal{Z} . Then the unforced system (9) is incrementally exponentially stable (IES) on \mathcal{Z} .

The previous theorem is an immediate consequence of exponential stability of the equilibrium point on a compact invariant set. Since excitable systems are not necessarily uniformly contractive with respect to the input [11], [19], contraction may not be preserved if an input is applied. However, as the next theorem will show, for the class of inputs (3) contraction is preserved, provided that the events in the train are, on average, sufficiently spread in time. The theorem builds on classical average dwell-time arguments [20], [21].

Theorem 2 (IES under average dwell time). By Theorem 1, there exist $k \ge 1$ and $\lambda > 0$ such that, for all $t_2 \ge t_1 \ge 0$ and all $z_1, z_2 \in \mathcal{Z}$,

$$\|\varphi(t_2, z_1) - \varphi(t_2, z_2)\| \le k e^{-\lambda(t_2 - t_1)} \|\varphi(t_1, z_1) - \varphi(t_1, z_2)\|.$$

Let u be the impulse train (3). If the impulse times satisfy the average dwell-time bound

$$N(t_2, t_1) \le N_0 + \frac{t_2 - t_1}{\tau_a}, \quad \forall t_2 \ge t_1 \ge 0,$$

with N_0 and τ_a independent of t_2, t_1 , then the forced system (9) under (3) is IES on \mathbb{Z} whenever

$$\lambda > \frac{\ln k}{\tau_a}$$
.

Proof. See Appendix.

Considering also the class of periodic signals, it is of particular interest to show how contraction depends on the signal period T.

Corollary 1 (Periodic impulse trains). *If the impulse train* (3) *is periodic with period* T > 0, *then the forced system is IES whenever*

$$\frac{1}{T} < \frac{\lambda}{\ln k}.$$

Proof. See Appendix.

For a periodic train with inter-impulse period T, if the rate of arrivals of the impulses is below the margin $\lambda/\ln k$, the exponential convergence between any two trajectories of the forced system survives. As T decreases, the bound eventually fails, matching the intuition that very high-rate pulsing undermines contractivity, since the synapse tends to be always open, as proved in the following lemma.

Lemma 3 (High–rate periodic impulses keep the synapse open). Let (2) be driven by (3) with impulse times $t_{\ell} = \ell T$, T > 0. For each T > 0 there exists a unique T-periodic solution $s_*^{(T)}$ of (2) forced by (3), which is globally exponentially attractive. Moreover, for every L > 0 and every $\phi \in L^1([0, L])$,

$$\lim_{T \to 0} \int_0^L \phi(t) \left(s_*^{(T)}(t) - 1 \right) dt = 0,$$

that is, $s_*^{(T)} \rightharpoonup 1$ weakly on compact intervals as $T \to 0$.

Lemma 3 shows that, for $T \to 0$ the synaptic state approaches a constant value 1. The intuition behind is that, for impulses arriving at very high rate, system (9) behaves, on compact intervals of time, in the same way as it were subject to a constant input $v_{\rm pre}$. Thus, in view of [22, Thm. 1], this "tonic limit" destabilizes the rest state and creates a limit cycle, explaining the loss of the contraction margin in Theorem 2 as $T \to 0$.

Simulations illustrating these results are shown in Figure 3. When impulses are too close together, they approximate a constant current that can induce a limit cycle. Trajectories then do not converge to a common steady-state response, the phase shift from different initial conditions persists, and the behavior is not reliable. By contrast, sufficiently sparse periodic impulses yield a unique and attractive steady-state response, which implies reliable behavior. These observations align with [11], where contraction of the forced system is linked to an average-time condition stating that trajectories must spend enough time in a contractive region to synchronize asymptotically.

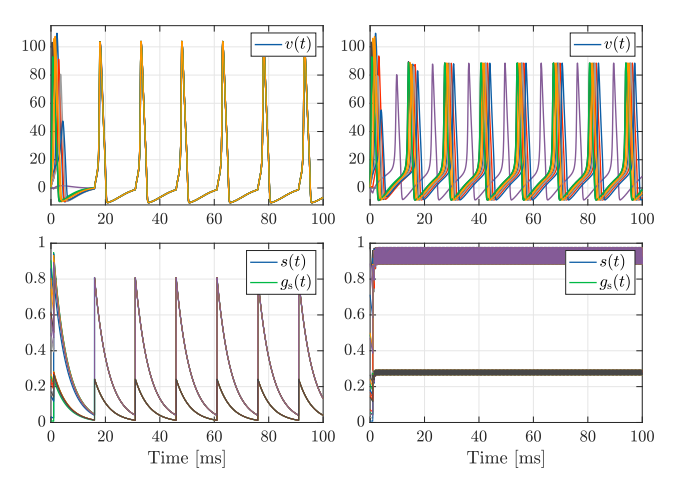


Fig. 3: Hodgkin–Huxley neuron driven by periodic impulse trains. Top: membrane voltage for multiple initial conditions under the same input. Bottom: synaptic state s(t) and conductance $g_{\rm s}(t)$. Left column (sparse, $T=15\,{\rm ms}$): contraction is preserved and all trajectories converge to a unique steady-state response. Right column (dense, $T=0.5\,{\rm ms}$): the synapse is effectively always open (constant input), a limit cycle emerges, and phase offsets persist across initial conditions. ($\alpha=0.8,\ \tau_s=5\,{\rm ms},\ \bar{g}_s=0.3\,{\rm mS/cm^2},\ E_{\rm s}=65\,{\rm mV}$).

IV. EVENT RELIABILITY

Reliability is a property of the discrete event map, yet in our setting it is inherited directly from contraction of the continuous dynamics [11]. If (9) is contractive on the compact forward–invariant set \mathcal{Z} , then for any fixed input sequence $\mathcal{I} \in \mathbb{U}$ and fixed parameters the corresponding trajectories $\varphi(t,z_0,\mathcal{I})$ converge to the same steady–state response. By means of the event detector (10), the event sets extracted from these trajectories align asymptotically. In this sense, contraction of the flow implies reliability of spike times

Moreover, the robustness inherited by contraction carries over to events. Under bounded disturbances or small parameter variations across trials, incremental exponential stability yields uniform trajectory bounds that scale with the perturbation magnitude. Consequently, the induced timing errors remain uniformly *bounded* after a transient. In contrast, when the flow is not contractive, differences in initial conditions or parameters can lead to persistent phase offsets and highly variable spike timings.

In practice, the threshold $v_{\rm high}$ is chosen inside the spike excursion where the upstroke is monotone, and a value near $(E_{\rm min}+E_{\rm max})/2$ often suffices. In planar excitable systems (e.g., FitzHugh–Nagumo or Morris–Lecar [23], [24]), this corresponds to placing $v_{\rm high}$ just above the upper knee of the fast–variable nullcline, where the trajectory jumps to the excited branch and crosses the threshold exactly once with positive slope.

A simulation illustrating these points is shown in Figure 4. The neuron is driven by the same random impulse

train across trials while initial conditions, and parameters. When contraction of the underlying dynamics is preserved, trajectories remain uniformly close after a transient despite these perturbations, and the extracted event sequences align up to a small bounded timing error. In the non–contractive regime, by contrast, trial–to–trial phase differences persist and spike times vary consistently.

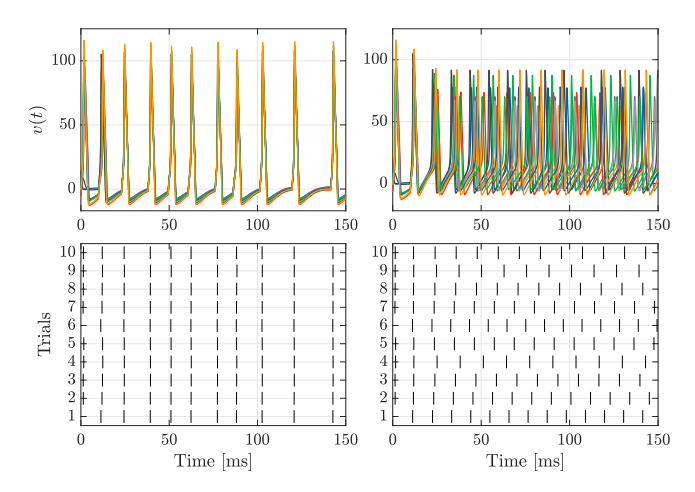


Fig. 4: Hodgkin–Huxley neuron with a conductance synapse driven by two impulse trains. Top: membrane voltage from 10 trials under the same input, with random initial condition and parameters perturbed by $\pm 20\%$ of baseline values. Bottom: spike raster plots. Left column (sparse): a random train with dead-time yields tightly aligned spike times across trials. Right column (dense): a uniform train with period $T=0.01\,\mathrm{ms}$ keeps the synapse effectively open, producing an almost constant conductance, with trajectories showing tonic-like activity with trial-dependent phase. (Baseline parameters: $\alpha=1,~\tau_s=4\,\mathrm{ms},~\bar{g}_s=0.425\,\mathrm{mS/cm^2},~E_s=65\,\mathrm{mV}).$

V. DISCUSSION

A. Rate vs spike code

A long-standing distinction in neural coding contrasts spike-code and rate-code views [25]. In a spike-based view, precise event times are meaningful for computational purposes. in a rate-code view, the firing rate is taken as the fundamental signal, effectively averaging over spikes and discarding timing precision. Our contraction-based analysis provides a concrete mathematical counterpart to this distinction. When the flow is contractive, repeated trials yield nearidentical spike trains after a transient, so timing becomes reproducible and robust and can serve as a reliable carrier of information. In non-contractive regimes, tiny variations in initial conditions or perturbations produce persistent phase differences and divergent spike patterns across trials. In that case the only consistent signal is the average firing rate measured over time or trials. In short, contraction identifies when precise spike timing can function as the signal, whereas lack of contraction forces a retreat to coarse-grained, ratelevel descriptions.

B. Endogenous vs exogenous oscillators

Mathematical models of rhythm generation often fall into two distinct categories: endogenous oscillators and exogenous oscillators. Endogenous oscillators are modelled as limit cycle oscillations of autonomous differential equations [26]. They oscillate without any external input. Exogenous oscillators are modelled as contractive systems entrained by oscillatory inputs [27]. They cannot oscillate without external input. Endogenous oscillators are not reliable because autonomous limit cycles are phase sensitive [26]. Exogeneous oscillators do not resonate because they lack internal resonance mechanisms.

Excitable systems borrow the best of the two worlds. They are exogenous, because they do not oscillate without external inputs. But they are also endogenous, because the mechanism of their oscillations is purely internal. The only role of the external input is to entrain the internal rhythm in a reliable manner.

VI. CONCLUSIONS

This paper has studied the contraction properties of conductance-based models of excitability. Contraction is an essential continuity property of the continuous-time behavior for the reliability of the discrete event timings. On the continuous side, we established incremental exponential stability of the unforced Hodgkin-Huxley dynamics on a compact forward-invariant set. Under impulsive forcing, we showed that contraction is preserved when impulses are sufficiently spaced in time, with an explicit sufficient condition for periodic drives. At the opposite extreme, we characterized the high-rate limit: the synapse behaves as effectively always open, the dynamics approach a constant-conductance regime, and a limit cycle can emerge, thereby eroding the contraction margin. This reconciles the robustness of forced, contractive responses with the fragility inherent to autonomous oscillations. On the discrete side, reliability follows directly from contraction. With an event detector that yields isolated events, contraction makes trajectories converge after a transient, and the detected spikes do as well. The same mechanism explains robustness across trials: bounded disturbances and small parameter variations yield uniformly bounded trajectory deviations and, hence, uniformly bounded timing errors. Simulations with randomized initial conditions and parameter and kinetic perturbations illustrate both outcomes: sparse inputs lead to a unique steady response and reliable spike timing, whereas dense inputs induce tonic activity and loss of timing reliability.

Beyond methodology, the results clarify coding viewpoints: in contractive regimes, precise spike timing can serve as a stable information carrier, whereas in non-contractive regimes persistent phase variability undermines timing reproducibility and a rate-based description becomes the meaningful one.

Future work will extend the framework to general conductance-based neuron models with diverse ionic currents, incorporate richer synaptic dynamics and input classes, and address networks of excitable systems.

APPENDIX

Proof of Lemma 1. Consider $v_{\text{pre}}(t)$ as in (3). Between impulses the synapse dynamics obeys $\dot{s} = -(1/\tau_s)s$, so one has

$$s(t) = s(t_{\ell}^{+}) e^{-(t-t_{\ell})/\tau_{s}}, \quad \forall t \in [t_{\ell}, t_{\ell+1}).$$
 (12)

At an impulse time t_{ℓ} , the jump condition obtained by integrating (2) across t_{ℓ} is

$$s(t_{\ell}^{+}) = s(t_{\ell}^{-}) + \alpha (1 - s(t_{\ell}^{-})) = (1 - \alpha)s(t_{\ell}^{-}) + \alpha.$$

Assume $s(t_{\ell}^{-}) \in [0, 1]$, then $s(t_{\ell}^{+}) \in [0, 1]$.

Moreover, because of (12), if $s(t_{\ell}^+) \in [0,1]$, then $s(t) \in [0,1] \ \forall t \in [t_{\ell}, t_{\ell} + 1)$. Therefore S is forward invariant for (2).

The gate dynamics evolve on \mathcal{X} . Evaluating the vector field describing the dynamics at the boundaries $x_j \in \{0, 1\}$ gives

$$\begin{aligned} x_j &= 0 \,:\, \tau_j(v) \dot{x}_j = \mu_j(v) \implies \dot{x}_j > 0, \\ x_j &= 1 \,:\, \tau_j(v) \dot{x}_j = \mu_j(v) - 1 \implies \dot{x}_j < 0, \end{aligned}$$

for all $j \in \{1, ..., m\}$ and any v. For the voltage, at the boundaries $v \in \{E_{\min}, E_{\max}\}$ we have

$$C\dot{v} = -G(x) \left(E_{\min} - E(x) \right) > 0,$$

$$C\dot{v} = -G(x) \left(E_{\max} - E(x) \right) < 0,$$

for any $x = col(x_1, ..., x_m)$. Therefore, \mathcal{Z} is forward invariant for (1).

Proof of Lemma 2. Consider system (9) with $u\equiv 0,\,z_0\in\mathcal{Z}$, and let $\varphi(t,z_0)$ be the solution. By Assumption 1, local exponential stability of z^* implies the existence of r>0, $\lambda>0$, and $c\geq 1$ such that

$$\|\varphi(t, z_0) - z^*\| \le ce^{-\lambda t} \|z_0 - z^*\|, \quad \forall z_0 \in B_r(z^*),$$
 (13)

for all $t \geq 0$, where $B_r(z^*) := \{z \in \mathcal{Z} : ||z - z^*|| < r\}$. Since (9) is time invariant, attractiveness of z^* is uniform, hence there exists $T^* > 0$ such that

$$\varphi(t, z_0) \in B_r(z^*), \quad \forall z_0 \in \mathcal{Z}, \ \forall t > T^*.$$

Set $R := \sup_{\xi \in \mathcal{Z}} \|\xi - z^*\| < \infty$. If $\|z_0 - z^*\| \le r$, then

$$\|\varphi(t, z_0) - z^*\| \le ce^{-\lambda t} \|z_0 - z^*\|, \quad \forall t \ge 0.$$

If $||z_0 - z^*|| > r$, then for $t \in [0, T^*]$,

$$\|\varphi(t,z_0) - z^*\| \le R \le \frac{R}{r} \|z_0 - z^*\| \le \frac{R}{r} e^{\lambda T^*} e^{-\lambda t} \|z_0 - z^*\|.$$

For $t > T^*$, applying (13) from time T^* yields

$$\|\varphi(t,z_0) - z^*\| \le c \frac{R}{r} e^{\lambda T^*} e^{-\lambda t} \|z_0 - z^*\|.$$

Therefore, with $K\coloneqq \max\{c,\frac{R}{r}e^{\lambda T^*},c\frac{R}{r}e^{\lambda T^*}\}$ we obtain, for all $z_0\in\mathcal{Z},$

$$\|\varphi(t, z_0) - z^*\| \le Ke^{-\lambda t} \|z_0 - z^*\|, \quad \forall t \ge 0.$$

Thus z^* is exponentially stable on \mathcal{Z} .

Proof of Theorem 1. Let $\varphi(t, z_0)$ be a solution of (9) with $u \equiv 0$ from $z_0 \in \mathcal{Z}$, and let DF(z) be its Jacobian. Local

exponential stability of z^{\ast} implies the existence of $P,Q\succ 0$ and r>0 such that

$$DF(z)^{\top}P + PDF(z) \le -Q, \quad \forall z \in B_r^{\|\cdot\|_P}(z^*),$$

which implies contraction in the P-metric (see [8, Thm 2.29]). By norm equivalence, there exist m, M > 0 such that $m\|\xi\| \le \|\xi\|_P \le M\|\xi\|$ for all ξ . Hence

$$B_{r/M}(z^*) \subseteq B_r^{\|\cdot\|_P}(z^*) \subseteq B_{r/m}(z^*).$$

Let $\bar{r}:=r/M.$ Then by converting the P-metric estimate to the Euclidean norm we obtain constants $\lambda>0$ and $c\geq 1$ such that

$$\|\varphi(t,x_0)-\varphi(t,y_0)\| \le ce^{-\lambda t}\|x_0-y_0\|, \quad \forall x_0,y_0 \in B_{\bar{r}}(z^*).$$
(14)

Uniform attractivity of z^* on $\mathcal Z$ yields $T^*>0$ such that $\varphi(t,z_0)\in B_{\bar r}(z^*)$ for all $t>T^*$ and all $z_0\in \mathcal Z$. For arbitrary $x_0,y_0\in \mathcal Z$, set $\Delta(t):=\varphi(t,x_0)-\varphi(t,y_0)$. Since f is C^1 on $\mathcal Z$, there exists L>0 such that

$$||f(p) - f(q)|| \le L||p - q||, \quad \forall p, q \in \mathcal{Z}.$$

Thus, for $t \in [0, T^*]$, it holds

$$\frac{d}{dt} \frac{1}{2} ||\Delta(t)||^2 = \langle \Delta(t), f(\varphi(t, x_0)) - f(\varphi(t, y_0)) \rangle$$

$$\leq L ||\Delta(t)||^2,$$

hence by the Grönwall Lemma

$$\|\Delta(t)\| \le e^{Lt} \|x_0 - y_0\|, \quad t \in [0, T^*].$$

For $t \geq T^*$, (14) gives

$$\|\Delta(t)\| \le ce^{-\lambda(t-T^*)} \|\Delta(T^*)\|.$$

Combining the two estimates, we obtain

$$\|\Delta(t)\| \le ce^{-\lambda(t-T^*)}e^{LT^*} \|x_0 - y_0\|$$

$$= ce^{\lambda T^*}e^{-\lambda t}e^{LT^*} \|x_0 - y_0\|$$

$$= Ke^{-\lambda t} \|x_0 - y_0\|,$$

for $t \geq 0$, and with $K \coloneqq ce^{(L+\lambda)T^*}$. Then, the unforced system is IES on \mathcal{Z} .

Proof of Theorem 2. Fix $t_2 \geq t_1 \geq 0$ and two solutions $\varphi(\cdot, x_0, u)$, $\varphi(\cdot, y_0, u)$ under the same input u given by (3). Let $\Sigma \subset \mathbb{R}_+$ be the set of impulse times, and list those lying in $(t_1, t_2]$ as

$$\sigma_1 < \dots < \sigma_N$$
, $N := \operatorname{card} \{ \sigma \in \Sigma : t_1 < \sigma \le t_2 \} \in \mathbb{N}_0$.

Define the partition

$$\rho_0 := t_1, \qquad \rho_i := \sigma_i \ (i = 1, \dots, N), \qquad \rho_{N+1} := t_2.$$

Set $\Delta(t) := \varphi(t, x_0, u) - \varphi(t, y_0, u)$. On each flow segment $[\rho_i, \rho_{i+1})$ there are no impulses, so by Theorem 1 we have

$$\|\Delta(\rho_{i+1}^-)\| \le k e^{-\lambda(\rho_{i+1}-\rho_i)} \|\Delta(\rho_i^+)\|.$$

At each impulse $\sigma_i = \rho_i$ only s jumps as $s^+ = (1-\alpha)s^- + \alpha$ with $\alpha \in (0,1]$, so

$$\|\Delta(\rho_i^+)\| \le \|\Delta(\rho_i^-)\|.$$

Chaining these N jumps and N+1 flow segments yields

$$\|\Delta(t_2)\| = \|\Delta(\rho_{N+1}^-)\| \le \left(\prod_{i=0}^N k e^{-\lambda(\rho_{i+1}-\rho_i)}\right) \|\Delta(t_1)\|$$
$$= k^{N+1} e^{-\lambda(t_2-t_1)} \|\Delta(t_1)\|.$$

By the interval average dwell-time bound, $N \leq N_0 + \frac{t_2 - t_1}{\tau_a}$, hence

$$k^{N+1} \le k^{N_0+1} e^{\frac{\ln k}{\tau_a}(t_2-t_1)}$$
.

Therefore

$$\|\Delta(t_2)\| \le k^{N_0+1} e^{-\left(\lambda - \frac{\ln k}{\tau_a}\right)(t_2 - t_1)} \|\Delta(t_1)\|, \quad \forall t_2 \ge t_1 \ge 0.$$

If $\lambda > \frac{\ln k}{\tau_a}$ the rate is positive, and the claim follows.

Proof of Corollary 1. Let $\Sigma = \{t_{\ell} = \ell T : \ell \in \mathbb{N}\}$. For any $t_2 \geq t_1 \geq 0$ let

$$N := \operatorname{card} \{ \sigma \in \Sigma : t_1 < \sigma \le t_2 \}.$$

Since $t_{\ell+1}-t_\ell=T$, we have $N\leq 1+\frac{t_2-t_1}{T}$. Hence, the average dwell-time condition of Theorem 2 holds with $\tau_a=T$ and $N_0=1$. Applying Theorem 2 gives IES provided $\lambda>\frac{\ln k}{\tau_a}=\frac{\ln k}{T}$, that is, $1/T<\lambda/\ln k$.

Proof of Lemma 3. From the proof of Lemma 1, for $t \in [t_{\ell}, t_{\ell+1})$,

$$s(t) = s(t_{\ell}^{+})e^{-(t-t_{\ell})/\tau_{s}},$$

and at impulse times t_{ℓ} ,

$$s(t_{\ell}^{+}) = (1 - \alpha)s(t_{\ell}^{-}) + \alpha.$$

Since the impulses are T-periodic, $t_{\ell+1} - t_{\ell} = T$. At $t_{\ell+1}$,

$$s_{\ell+1} = s(t_{\ell+1}^+) = (1 - \alpha)s(t_{\ell+1}^-) + \alpha,$$

and, by the flow on $[t_{\ell}, t_{\ell+1})$,

$$s(t_{\ell+1}^-) = e^{-T/\tau_s} s(t_{\ell}^+) = e^{-T/\tau_s} s_{\ell}.$$

Therefore

$$s_{\ell+1} = (1 - \alpha)e^{-T/\tau_s}s_{\ell} + \alpha =: a_T s_{\ell} + \alpha, \quad a_T \in [0, 1).$$

The affine map $s_{\ell+1} = a_T s_{\ell} + \alpha$ is a strict contraction and admits the unique fixed point

$$s_T^\star = \frac{\alpha}{1-a_T} = \frac{\alpha}{1-(1-\alpha)e^{-T/\tau_s}}.$$

Hence $s_{\ell} \to s_T^{\star}$ exponentially for any $s_0 \in [0,1]$. The corresponding T-periodic solution is

$$s_*^{(T)}(t) = s_T^* e^{-(t-\ell T)/\tau_s}, \qquad t \in [\ell T, (\ell+1)T).$$

Moreover, letting $\ell = |t/T|$, for $t \in [\ell T, (\ell+1)T)$,

$$|s(t) - s_*^{(T)}(t)| = |s_\ell - s_T^{\star}|e^{-(t-\ell T)/\tau_s}$$

$$\leq a_T^{\ell} e^{-(t-\ell T)/\tau_s} |s_0 - s_T^{\star}|$$

$$< a_T^{-1} e^{-\gamma_T t} |s_0 - s_T^{\star}|,$$

where $\gamma_T := -\frac{1}{T} \ln a_T > 0$ (we used $\ell \geq t/T - 1$ and $e^{-(t-\ell T)/\tau_s} \leq 1$). Then, $s_*^{(T)}$ is globally exponentially attractive.

To prove weak convergence of $s_*^{(T)}$ to 1, first note that for $t \in [\ell T, (\ell+1)T)$,

$$s_*^{(T)}(t) \in [s_T^{\star} e^{-T/\tau_s}, s_T^{\star}],$$

so

$$\sup_{t>0} |s_*^{(T)}(t) - 1| = \max\{1 - s_T^{\star} 1 - s_T^{\star} e^{-T/\tau_s}\}.$$

A direct calculation gives

$$1 - s_T^{\star} = \frac{(1 - \alpha)(1 - e^{-T/\tau_s})}{1 - (1 - \alpha)e^{-T/\tau_s}},$$
$$1 - s_T^{\star} e^{-T/\tau_s} = \frac{1 - e^{-T/\tau_s}}{1 - (1 - \alpha)e^{-T/\tau_s}}.$$

Using $1 - e^{-x} \le x$ for $x \ge 0$ and $1 - (1 - \alpha)e^{-T/\tau_s} \ge \alpha$, we obtain the uniform bound

$$\sup_{t>0} |s_*^{(T)}(t) - 1| \le \frac{T}{\alpha \tau_s} \xrightarrow[T \to 0]{} 0. \tag{15}$$

Therefore, for every L > 0 and every $\phi \in L^1([0, L])$,

$$\left| \int_0^L \phi(t) \left(s_*^{(T)}(t) - 1 \right) dt \right| \le \|\phi\|_{L^1} \sup_{t \in [0, L]} |s_*^{(T)}(t) - 1|$$

and hence, in view of (15), $s_*^{(T)} \to 1$ weakly on compact intervals as $T \to 0$.

REFERENCES

- [1] R. Sepulchre, "Spiking control systems," *Proceedings of the IEEE*, vol. 110, no. 5, pp. 577–589, 2022.
- [2] A. Cecconi, M. Bin, R. Sepulchre, and L. Marconi, "Event disturbance rejection: A case study," 2025, presented at 2025 NOLCOS, Reykjavik.
- [3] R. Sepulchre, A. Cecconi, M. Bin, and L. Marconi, "Regulation without calibration," arXiv preprint arXiv:2505.09515, 2025.
- [4] Z. F. Mainen and T. J. Sejnowski, "Reliability of Spike Timing in Neocortical Neurons," *Science*, vol. 268, no. 5216, pp. 1503–1506, 1995.
- [5] R. Brette and E. Guigon, "Reliability of Spike Timing Is a General Property of Spiking Model Neurons," *Neural Comput*, vol. 15, no. 2, pp. 279–308, 2003.
- [6] K. K. Lin, "Stimulus-Response Reliability of Biological Networks," in Nonautonomous Dynamical Systems in the Life Sciences, P. E. Kloeden and C. Pötzsche, Eds. Cham: Springer, 2013, pp. 135–161.
- [7] W. Lohmiller and J.-J. E. Slotine, "On Contraction Analysis for Nonlinear Systems," *Automatica*, vol. 34, no. 6, pp. 683–696, 1998.
- [8] A. Pavlov, N. van de Wouw, and H. Nijmeijer, Uniform Output Regulation of Nonlinear Systems. Boston, MA: Birkhäuser Boston, 2006.
- [9] F. Bullo, Contraction Theory for Dynamical Systems, 1st ed. Kindle Direct Publishing, 2024.
- [10] J. G. Lee, T. B. Burghi, and R. Sepulchre, "Open-loop contraction design," in 2022 IEEE 61st Conference on Decision and Control (CDC), 2022, pp. 7339–7345.
- [11] M. Bin, A. Čecconi, and L. Marconi, "Reliability entails inputselective contraction and regulation in excitable networks," 2025, arXiv:2511.02554
- [12] E. M. Izhikevich, Dynamical Systems in Neuroscience: The Geometry of Excitability and Bursting. The MIT Press, 2006.
- [13] G. B. Ermentrout and D. H. Terman, Mathematical Foundations of Neuroscience, ser. Interdisciplinary Applied Mathematics. New York, NY: Springer New York, 2010, vol. 35. [Online]. Available: http://link.springer.com/10.1007/978-0-387-87708-2
- [14] W. Gerstner, W. M. Kistler, R. Naud, and L. Paninski, Neuronal dynamics: From single neurons to networks and models of cognition. Cambridge University Press, 2014.

- [15] T. Medvedeva, A. Franci, and F. Castaños, "Formalizing neuromorphic control systems: A general proposal and a rhythmic case study," 2025, submitted to the IEEE Conference on Decision and Control (CDC), Rio de Janeiro, Brazil.
- [16] A. L. Hodgkin, "The local electric changes associated with repetitive action in a non-medullated axon," *The Journal of Physiology*, vol. 107, pp. 165–181, 1948.
- [17] E. M. Izhikevich, "Neural excitability, spiking and bursting," Int J Bifurc Chaos Appl Sci Eng, vol. 10, pp. 1171–1266, Jun. 2000.
- [18] B. S. Rüffer, N. van de Wouw, and M. Mueller, "Convergent systems vs. incremental stability," *Systems & Control Letters*, vol. 62, no. 3, pp. 277–285, 2013. [Online]. Available: https://www.sciencedirect.com/science/article/pii/S0167691112002393
- [19] J. Jouffroy, "A simple extension of contraction theory to study incremental stability properties." IEEE, 2003, pp. 1315–1321.
 [20] J. Hespanha and A. Morse, "Stability of switched systems with average
- [20] J. Hespanha and A. Morse, "Stability of switched systems with average dwell-time," in *Proceedings of the 38th IEEE Conference on Decision* and Control (Cat. No.99CH36304), vol. 3, 1999, pp. 2655–2660 vol.3.
- [21] D. Liberzon, Switching in systems and control. Springer, 2003, vol. 190.
- [22] E. D. Sontag, Mathematical control theory: deterministic finite dimensional systems. Springer Science & Business Media, 2013, vol. 6.
- [23] R. FitzHugh, "Impulses and Physiological States in Theoretical Models of Nerve Membrane," *Biophysical Journal*, vol. 1, no. 6, pp. 445–466, 1961.
- [24] C. Morris and H. Lecar, "Voltage oscillations in the barnacle giant muscle fiber," *Biophysical journal*, vol. 35, no. 1, pp. 193–213, 1981.
- [25] R. Brette, "Philosophy of the Spike: Rate-Based vs. Spike-Based Theories of the Brain," Front Syst Neurosci, vol. 9, 2015.
- [26] A. Pikovsky, M. G. Rosenblum, and J. Kurths, Synchronization: A Universal Concept in Nonlinear Sciences. Cambridge University Press, 2001.
- [27] E. D. Sontag, "Contractive systems with inputs," in Perspectives in Mathematical System Theory, Control, and Signal Processing: A Festschrift in Honor of Yutaka Yamamoto on the Occasion of his 60th Birthday. Springer, 2010, pp. 217–228.